# Electron Cloud Instability with Space Charge or Beam Beam

G. Rumolo and F. Zimmermann, CERN, Geneva, Switzerland

*Abstract*

Simulations of the single-bunch instability due to the electron cloud reveal a significant further destabilization, if a proton space-charge or beam-beam force is also taken into account, and a resulting qualitative change in the instability behaviour. The synergy between these phenomena is possibly consistent with a simplified analytical few-particle model, in which the effect of space charge (or beam-beam) is represented by a $z$-dependent parabolic betatron tune variation along the bunch, and that of the electron cloud by a constant transverse wake and a linear tune variation. We show that in this model the combination of electron cloud and space charge can sustain larger growth rates.

## 1 INTRODUCTION

In this report, we discuss the interplay between the single-bunch electron-cloud instability and a transverse space-charge force or beam-beam interaction. The only effect of space charge (or beam-beam) that we consider is the quadratic variation of the betatron tune with the longitudinal position along the bunch. Transversely the force is assumed to be perfectly linear.

In Section 2 we compare the results of multi-particle computer simulations for an LHC bunch in the CERN SPS which do or do not include the space-charge or beam-beam force. In the simulation, tune shift due to space-charge or beam-beam are treated differently. To model the space charge force, we apply on each turn an additional (incoherent) betatron rotation around the center of each longitudinal bunch slice. In the case of beam-beam, we instead rotate all particles around the bunch centroid, or around the closed orbit. In all cases, the rotation angle varies with the longitudinal position, according to the Gaussian beam profile.

In Section 3 we develop 3 and 4-particle models, by which we analytically study the combined effect of the electron cloud, represented by a constant dipole wake and a linear tune shift due to the electron pinch, and the space-charge tune shift. For ease of calculation, we approximate the Gaussian beam profile by an inverse parabola. We evaluate the final analytical expressions for the CERN SPS.

Results are summarized and conclusions are drawn in Section 4.

## 2 SIMULATIONS

The effect of the electron cloud on the single bunch stability is modelled by a dedicated simulation program, called HEADTAIL [1]. This simulation code studies the turn-by-turn interaction of a single bunch with an electron cloud, which is assumed to be produced by the preceding bunches. Both the bunch and the electrons are modelled by macroparticles. The electric force that the electrons experience during the beam passage as well as the converse forces that the electrons exert on various longitudinal slices of the beam are computed using a PIC module. The interaction between electrons and the beam is computed successively for different longitudinal slices of the bunch.

In the simulation, the interaction between the beam and the electrons occurs at one or more locations of the ring. In between the beam is propagated around the arcs of the storage ring. The betatron motion in both planes is modelled by a rotation matrix. On each turn the bunch interacts with a new, unperturbed electron distribution. The synchrotron motion is included and the beam macro particles slowly rotate in synchrotron phase space and interchange their longitudinal positions. The effect of chromaticity is modelled by an additional rotation matrix which depends on the energy of each particle. Finally, a regular transverse impedance, represented by a broadband resonator, as well as a proton space-charge force or beam-beam interaction can optionally be taken into account.

More precisely, we model the transverse motion of macroelectrons as follows. At each passage through the electron cloud a particle of the bunch receives both a vertical and a horizontal deflection, $\Delta x'$ and $\Delta y'$, which, if selected, include the effect of the broadband impedance as well. The particles are next propagated through the ring, by means of (1) a matrix $\mathbf{M}_{\rm ring}$ describing the nominal phase advance as determined by the betatron tune, (2) a matrix $\mathbf{M}_{\rm chr}$ modelling the effect of chromaticity and depending on the particle's momentum, and (3) a space-charge rotation which varies with the particle's longitudinal position, according to the longitudinal density profile of the bunch. The space-charge rotation is performed around the center of a bunch slice, the other two around the closed orbit. Thus, the total horizontal transformation from turn $n$ to turn $(n+1)$ is

$$\begin{pmatrix} x_{n+1} \\ x'_{n+1} \end{pmatrix} = \mathbf{M}_{\rm chr}(\Delta p)\,\mathbf{M}_{\rm ring}$$
$$\left[\mathbf{M}_{sc}(z)\begin{pmatrix} x_n - \bar{x}(z) \\ x'_n + \Delta x' - \bar{x}'(z) \end{pmatrix} + \begin{pmatrix} \bar(x)(z) \\ \bar{x}'(z) \end{pmatrix}\right], \quad (1)$$

and the corresponding transformation is applied in the vertical plane. On each turn the beam macroparticles are regrouped into longitudinal slices, whose average sizes and centroid positions are calculated.

We have performed a series of simulations for the LHC beam at injection into the SPS. Table 1 lists the bunch parameters assumed, and table 2 gives further simulation parameters.

Figures 1–5 present the simulated beam size increase and centroid motion for an LHC bunch passing for 500 turns through the SPS. The figures refer to different representations of the space-charge or beam-beam force. In the simulation of Fig. 1 only the effect of the electron cloud is considered in addition to the linear ring optics. In the second simulation, illustrated in Fig. 2, the effect of a constant proton-space charge at 26 GeV is taken into account as well. Comparison of Figs. 1 and 2 reveals that the space charge renders the beam motion more unstable and more violent. In particular, it leads to slice centroid oscillations inside the bunch. On the other hand, the simulation without space charge shows a persistent emittance growth, more or less uniform along the bunch.

For the simulation reported in Fig. 2, the tune variation due to space charge was computed from the initial transverse beam size, neglecting the beam-size growth as a result of the instability. Since the bunch transverse size sensibly increases over the simulated 500 turns, another simulation was run where always the actual local beam size of each bunch slice was assumed in the computation of the space-charge force, with results as shown in Fig. 3. The growing beam size reduces the space-charge force at later times, and almost completely suppresses the coherent motion of the bunch centroid.

Figure 4 is the same as Fig. 2, except that the additional space-charge rotation was applied around the centroid of the bunch and not around the center of each bunch slice. This would model the effect of a hypothetical proton-proton beam-beam collision. This case was included to determine whether the rotation center is of importance, and the comparison of Figs. 4 and 2 suggests it is. Figure 4 shows less perturbations inside the bunch, but large centroid oscillations. Finally, Fig. 5 is the same as Fig. 4, except that it uses the instantaneous average beam size over the bunch for computing the beam-beam tune shift. As a result the centroid motion, which was visible in Fig. 4, has almost disappeared. This last case might approximate a situation as in KEKB, where the beam size of the opposing (electron) beam is always matched by an automatic feedback to the beam size of the positron beam, which is blown up by the electron cloud. As in Fig. 4 the tune-shift rotation is performed around the bunch centroid instead of the slice center. However, a more realistic simulation of the beam-beam force would rotate around the closed orbit.

The different signatures of the simulated instabilities might explain differences between the actual beam observations at SPS and KEKB, since at the SPS injection momentum of 26 GeV/c the beam is still affected by space charge forces.

Table 1: SPS parameters.

| variable | symbol | value |
|---|---|---|
| bunch population | $N_b$ | $10^{11}$ |
| beam momentum | $p$ | 26 GeV/c |
| circumference | $C$ | 6900 m |
| synchrotron frequency | $f_s$ | 200 Hz |
| beam momentum | $p$ | 26 GeV/c |
| electron-cloud density | $\rho_e$ | $10^{12}$ m$^{-3}$ |
| rms bunch length | $\sigma_z$ | 30 cm |
| rms energy spread | $\sigma_\delta$ | 0.002 |
| betatron tunes | $Q_{x,y}$ | 26.6 |
| average beta function | $\beta_{x,y}$ | 40 m |
| rms hor. beam size | $\sigma_x$ | 3 mm |
| rms vert. beam size | $\sigma_x$ | 2.3 mm |
| hor. & vert. chromaticity | $\xi_{x,y}$ | 0 |
| tune shift due to el. cloud | $\Delta Q_{\rm ec}$ | 0.0077 |
| space-charge tune shift | $\Delta Q_{\rm sc}$ | $-0.0365$ |
| wake field | — | none |

Table 2: Simulation parameters.

| variable | value |
|---|---|
| Size of the electron cloud | $20\sigma_x \times 20\sigma_y$ |
| Size of the grid | $1.1\times$ cloud |
| Number of horizontal cells | 128 |
| Number of vertical cells | 128 |
| number of macroparticles | $3\times10^5$ |
| number of macro-electrons | $10^5$ |
| number of bunch slices | 50 |
| longitudinal extent of bunch | 1.2 m |
| longitudinal profile | Gaussian |
| number of ep interactions per turn | 1 |

## 3 3 AND 4-PARTICLE MODELS

In this section, we construct a few-particle model, in order to study the interplay of space charge forces and the electron cloud. This model includes the two primary effects of the electron cloud, which is (1) a transverse wake field excited by transverse displacement between head and tail of the bunch, and (2) a positive tune shift which increases almost linear along the bunch. We now make the assumption that the further ingredient introduced by the space-charge force (or equivalently by a beam-beam interaction), is an additional variation of the betatron tune along the bunch. Ignoring transverse nonlinearities, we assume that the space-charge betatron tune shift only depends on the longitudinal coordinate, and for simplicity we approximate the bunch profile by an inverse parabola.

A two particle-model does not predict a head-tail instability caused by the variation of the tune as a function of longitudinal position. The situation here is different from the regular head-tail instability at nonzero chromaticity. In the latter case the betatron tune varies with momentum deviation $\delta$, whereas here it depends on $z$. According to Ref. [4] (see the footnote on page 198) for a $z$-dependent tune no instability is expected from a 2-particle model. This is because there is no net head-tail phase shift over

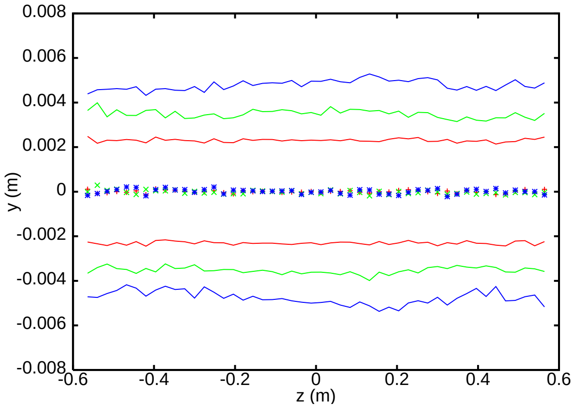


Figure 1: Simulated vertical bunch shape (centroid and rms beam size) after 0, 250, and 500 turns in the CERN SPS assuming an electron cloud density $\rho_e = 10^{12}$ m$^{-3}$ without proton space charge.

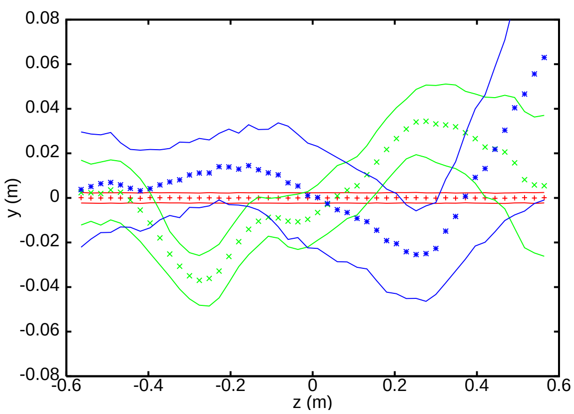


Figure 2: Simulated vertical bunch shape (centroid and rms beam size) after 0, 250, and 500 turns in the CERN SPS assuming an electron cloud density $\rho_e = 10^{12}$ m$^{-3}$ with proton space charge at 26 GeV/c. In this simulation, the space-charge force is computed from the initial beam size.

the half period of oscillations where one particles is trailing behind the other. In order to model the instability we must consider 3 or more particles, where we do have a net phase advance between the different particles. Such usage of a multi-particle to model the single-bunch electron-cloud effects was proposed by K. Cornelis [5].

In the following we first describe a 3-particle model, and then extend it to 4-particles in order to study the variation with particle number.

### *3.1 3 Particles*

The bunch is modelled by 3 particles, distributed with a constant oscillation amplitude $\hat{z}$ and uniform spacing in synchrotron phase space. We assume that each model particle carries a charge $N_b e/3$ and that particles excite a constant wake force $W_0$, which affects those following be-

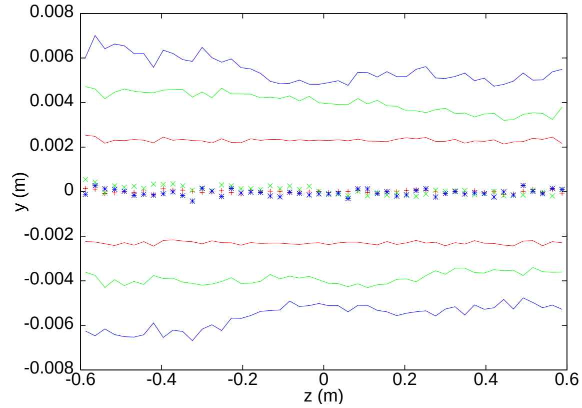


Figure 3: Simulated vertical bunch shape (centroid and rms beam size) after 0, 250, and 500 turns in the CERN SPS assuming an electron cloud density $\rho_e = 10^{12}$ m$^{-3}$ with proton space charge at 26 GeV/c. In this simulation, the space-charge force is computed from the actual local beam size.

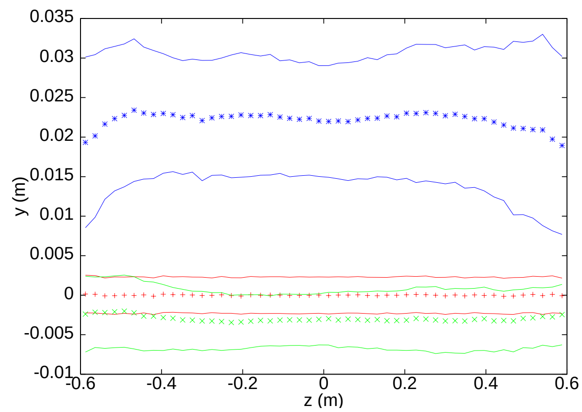


Figure 4: Simulated vertical bunch shape (centroid and rms beam size) after 0, 250, and 500 turns in the CERN SPS assuming an electron cloud density $\rho_e = 10^{12}$ m$^{-3}$ with a hypothetical pp beam-beam interaction of $\xi = -0.037$. The beam-beam force is computed from the initial beam size.

hind. This is of course a simplified description, and a refined analysis should take into account the strong variation of the wake with distance and with the longitudinal position. Some particles exchange their position every 6th synchrotron period, where the average phases of different particles are different.

The longitudinal positions of the particles evolve as

$$z_1 = \hat{z}\cos\left(\frac{\omega_s s}{c}\right) \tag{2}$$

$$z_2 = \hat{z}\cos\left(\frac{\omega_s s}{c} + \frac{2\pi}{3}\right) \tag{3}$$

$$z_3 = \hat{z}\cos\left(\frac{\omega_s s}{c} + \frac{4\pi}{3}\right) \tag{4}$$

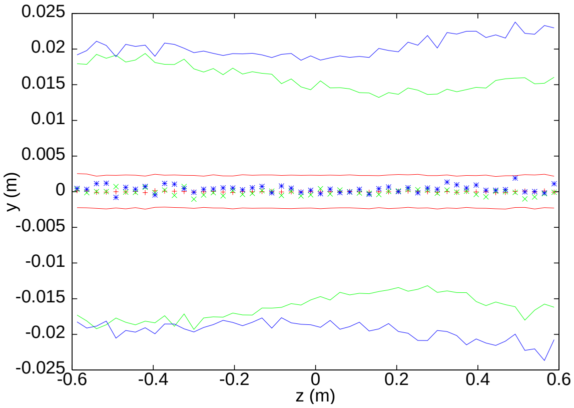


Figure 5: Simulated vertical bunch shape (centroid and rms beam size) after 0, 250, and 500 turns in the CERN SPS assuming an electron cloud density $\rho_e = 10^{12}$ m$^{-3}$ with a hypothetical pp beam-beam interaction of $\xi = -0.037$. The beam-beam force is computed from the actual average beam size.

where $\hat{z} \approx \sigma_z$. Positive $z$ indicates a position in front of the bunch center.

We approximate the dependence of the angular betatron frequency on the longitudinal position $z$ as

$$\begin{aligned} \omega_\beta(z) &= \omega_{\beta,0}\left[1-\left(\frac{\Delta\omega_\beta}{\omega_\beta}\right)_{\rm ec}\frac{z}{\hat{z}}-\left(\frac{\Delta\omega_\beta}{\omega_\beta}\right)_{\rm sc}\frac{z^2}{\hat{z}^2}\right] \\ &\equiv \omega_{\beta,0}\left(1-a\frac{z}{\hat{z}}-b\frac{z^2}{\hat{z}^2}\right), \end{aligned} \tag{5}$$

where the first linear term represents the effect of the electron cloud, the second quadratic one the space-charge force, and we have introduced coefficients, which represent the maximum relative tune shift from electron cloud and space charge, respectively.

Considering free betatron oscillations, the betatron phases $\phi_i$ of the three particles are obtained by integration

$$\begin{aligned} \phi_i(s) &= \omega_{\beta,0}\frac{s}{c}-\int_0^s ds\left[a\cos\left(\frac{\omega_s s}{c}+\phi_{i,0}\right)\right. && (6)\\ &\quad\left.+b\cos^2\left(\frac{\omega_s s}{c}+\phi_{i,0}\right)\right] \\ &= \omega_{\beta,0}\frac{s}{c}-\frac{bs\omega_{\beta,0}}{2c} && (7)\\ &\quad-\frac{a\omega_{\beta,0}}{\omega_s c}\sin\left(\frac{\omega_s s}{c}+\phi_{i,0}\right) && (8)\\ &\quad-\frac{b\omega_{\beta,0}}{4\omega_s c}\sin\left(\frac{2\omega_s s}{c}+2\phi_{i,0}\right) \\ &\equiv \omega_\beta\frac{s}{c}+\Delta\phi_i(s). && (9) \end{aligned}$$

We have absorbed the non-oscillating term in the average betatron phase advance $\bar{\omega}_\beta\frac{s}{c}$,

$$\bar{\omega}_\beta \equiv \omega_{\beta,0}-\frac{b\omega_{\beta,0}}{2}, \tag{10}$$

and introduce the oscillating part of the phase as

$$\begin{aligned} \Delta\phi_i(s) &\equiv -\frac{a\omega_{\beta,0}}{\omega_s}\sin\left(\frac{\omega_s s}{c}+\phi_{i,0}\right) \\ &\quad-\frac{b\omega_{\beta,0}}{4\omega_s}\sin\left(\frac{2\omega_s s}{c}+2\phi_{i,0}\right). \end{aligned} \tag{11}$$

Including the wake field, the betatron equation of motion for the $n$th particle is

$$y_n''+\left[\frac{\omega_\beta(z)}{c}\right]^2 y_n=\sum_{n',z_{n'}>z_n}\frac{N_b r_0 W_0}{3\gamma C}\,y_{n'} \tag{12}$$

where the sum extends of the particles in front of particle $n$.

We need to evaluate the equations of motion for a third period of the synchrotron oscillation. The solutions for the other two thirds then simply follow by cyclic permutation. The initial ordering of the particles is (1,3,2), *i.e.*, by which we indicate that the first particle is in front, followed by particle no. 3, and particle 2 is at the end. After a sixth period it changes to (3,1,2), and, thereafter, to (3,2,1), (2,3,1), (2,1,3), and (1,2,3). We solve the equation of motion for the first two sixths of a synchrotron period.

To this end, we write the solution for the $n$th particle as

$$y_n=\tilde{y}_n\exp\left[-i\phi_i(s)\right], \tag{13}$$

where the amplitude $\tilde{y}_n$ is assumed to be slowly varying due to the effect of the electron wake field.

Inserting (13) and the definition of $\phi_i(s)$, (9), into (12), we have

$$\tilde{y}_n'=\frac{iNr_0W_0c}{6\gamma C\omega_\beta}\sum_{n',z_{n'}>z_n}\tilde{y}_{n'}\exp\left[-i\Delta\phi_{n'}(s)+i\Delta\phi_n(s)\right] \tag{14}$$

For brevity we further abbreviate the coefficient by

$$D\equiv\frac{Nr_0W_0c}{6\gamma C\omega_\beta}. \tag{15}$$

Assuming that the phases $\Delta\phi_n(s)$ are much smaller than unity, we expand the exponential and can integrate the above equation to yield

$$\begin{aligned} \tilde{y}_n\left(\frac{T_s c}{6}\right) &\approx \tilde{y}_n(0)+iD\sum_{n',z_{n'}>z_n}\tilde{y}_{n'}\left[\frac{T_s c}{6}\right. \\ &\quad\left.-i\int_0^{T_s c/6}\left(\Delta\phi_{n'}(s)-\Delta\phi_n(s)\right)ds\right] \\ &\approx \tilde{y}_n+iD\sum_{n',z_{n'}>z_n}\tilde{y}_{n'}\left[\frac{\pi c}{3\omega_s}\right. \\ &\quad-i\left(\frac{a\omega_{\beta,0}c}{\omega_s^2}\right)\left[\cos\left(\pi/3+\phi_{n',0}\right)-\cos\phi_{n',0}\right] \\ &\quad-\frac{i}{8}\left(\frac{b\omega_{\beta,0}c}{\omega_s^2}\right)\left[\cos\left(2\pi/3+2\phi_{n',0}\right)-\cos 2\phi_{n',0}\right] \\ &\quad+i\left(\frac{a\omega_{\beta,0}c}{\omega_s^2}\right)\left[\cos\left(\pi/3+\phi_{n,0}\right)-\cos\phi_{n,0}\right] \\ &\quad\left.+\frac{i}{8}\left(\frac{b\omega_{\beta,0}c}{\omega_s^2}\right)\left[\cos\left(2\pi/3+2\phi_{n,0}\right)-\cos 2\phi_{n,0}\right]\right]. \end{aligned} \tag{16}$$

It was pointed out by K. Oide that this expansion and integration is only valid, if the phase differences $|\Delta\phi_{n'}(s) - \Delta\phi_n(s)|$ remain small compared with 1. Otherwise, the integration could be done numerically, possibly also including a more realistic shape of the wake field. For ease of notation, we introduce the three abbreviations

$$\bar{C} \equiv D\,\frac{\pi c}{3\omega_s} \tag{17}$$

$$\bar{A} \equiv D\,\frac{a\omega_{\beta,0}c}{\omega_s^2} \tag{18}$$

$$\bar{B} \equiv D\,\frac{b\omega_{\beta,0}c}{8\omega_s^2}, \tag{19}$$

where $\bar{A}$ refers to the tune shift from the electron cloud and $\bar{B}$ to that from the space charge. Explicitly, the Eq. (16) amounts to

$$\begin{aligned}
\tilde{y}_1(\pi/3) &\approx \tilde{y}_1(0)\\
\tilde{y}_3(\pi/3) &\approx \tilde{y}_3(0) + \tilde{y}_1(0)\left[i\bar{C} - \frac{3}{2}\bar{A} - \frac{3}{2}\bar{B}\right]\\
\tilde{y}_2(\pi/3) &\approx \tilde{y}_2(0) + \tilde{y}_1(0)\left[i\bar{C} - 3\bar{B}\right]\\
&\quad + \tilde{y}_3(0)\left[i\bar{C} + \frac{3}{2}\bar{A} - \frac{3}{2}\bar{B}\right]
\end{aligned} \tag{20}$$

The corresponding equations for the second sixth synchrotron period are

$$\begin{aligned}
\tilde{y}_3(2\pi/3) &\approx \tilde{y}_3(\pi/3)\\
\tilde{y}_1(2\pi/3) &\approx \tilde{y}_1(\pi/3) + \tilde{y}_3(0)\left[i\bar{C} + \frac{3}{2}\bar{A} + \frac{3}{2}\bar{B}\right]\\
\tilde{y}_2(2\pi/3) &\approx \tilde{y}_2(\pi/3) + \tilde{y}_3(\pi/3)\left[i\bar{C} + 3\bar{B}\right]\\
&\quad + \tilde{y}_1(\pi/3)\left[i\bar{C} - \frac{3}{2}\bar{A} + \frac{3}{2}\bar{B}\right].
\end{aligned} \tag{21}$$

We can rewrite these transformations as a matrix equations relating the initial and final 3-component amplitude vectors $\vec{y}(s) \equiv (\bar{y}_1(s), \bar{y}_2(s), \bar{y}_3(s))$,

$$\vec{y}(\pi/3) = \mathbf{M}_{\pi/3}\vec{y}(0) \tag{22}$$

and

$$\vec{y}(2\pi/3) = \mathbf{M}_{2\pi/3}\vec{y}(\pi/3). \tag{23}$$

According to Eqs. (20) and (21), the matrices $\mathbf{M}_{\pi/3}$ and $\mathbf{M}_{2\pi/3}$ are

$$\mathbf{M}_{\pi/3} = \begin{pmatrix} 1 & 0 & 0 \\ i\bar{C} - 3\bar{B} & 1 & i\bar{C} + \frac{3}{2}(\bar{A} - \bar{B}) \\ i\bar{C} - \frac{3}{2}(\bar{A} + \bar{B}) & 0 & 1 \end{pmatrix} \tag{24}$$

and

$$\mathbf{M}_{2\pi/3} = \begin{pmatrix} 1 & 0 & i\bar{C} + \frac{3}{2}(\bar{A} + \bar{B}) \\ i\bar{C} - \frac{3}{2}(\bar{A} - \bar{B}) & 1 & i\bar{C} + 3\bar{B} \\ 0 & 0 & 1 \end{pmatrix}. \tag{25}$$

After the second sixth synchrotron period the ordering of the 3 particles changes as $(3 \to 1)$, *i.e.*, now particle 3 is in front, $(2 \to 3)$, and $(1 \to 2)$, which is described by the permutation matrix

$$\mathbf{P} = \begin{pmatrix} 0 & 0 & 1 \\ 1 & 0 & 0 \\ 0 & 1 & 0 \end{pmatrix} \tag{26}$$

and the total matrix for one full synchrotron period is obtained by taking the 3rd power of the product matrix

$$\mathbf{M}_{\rm tot} \equiv (\mathbf{P}\mathbf{M}_{2\pi/3}\mathbf{M}_{\pi/3})^3. \tag{27}$$

In order to study the linear stability of this system, and to determine possible growth rates, it is sufficient to find the eigenvalues of the matrix

$$\mathbf{M}_{1/3} \equiv \mathbf{P}\mathbf{M}_{2\pi/3}\mathbf{M}_{\pi/3}. \tag{28}$$

Only keeping terms of first and second order in $\bar{A}$, $\bar{B}$, and $\bar{C}$, and also neglecting all higher-order cross products, we evaluate the matrix $\mathbf{M}_{1/3}$ as

$$\mathbf{M}_{1/3} \approx \begin{pmatrix} -\frac{3}{2}(\bar{A}+\bar{B}) + i\bar{C} & 0 & 1 \\ 1 - \frac{9}{4}(\bar{A}+\bar{B})^2 - \bar{C}^2 & 0 & \frac{3}{2}(\bar{A}+\bar{B}) + i\bar{C} \\ -\frac{3}{2}(\bar{A}+\bar{B}) + 2i\bar{C} + \bar{Y} & 1 & \frac{3}{2}(\bar{A}+\bar{B}) + 2i\bar{C} \end{pmatrix} \tag{29}$$

where

$$\bar{Y} \equiv \left(i\bar{C} + 3\bar{B}\right)\left(-\frac{3}{2}(\bar{A}+\bar{B}) + i\bar{C}\right) \tag{30}$$

The eigenvalues follow from the zeroes of the characteristic polynomial $p(\lambda)$,

$$\begin{aligned}
p(\lambda) &= 1 + \left(3i\bar{C} + 3i\bar{B}\bar{C} + \frac{9}{4}\bar{A}^2 + \frac{9}{4}\bar{B}^2 + \bar{C}^2\right)\lambda\\
&\quad + 3i\bar{C}\lambda^2 - \lambda^3
\end{aligned} \tag{31}$$

In the absence of an electron cloud, we have $\bar{X} = \bar{C} = 0$, the equation reduces to $(1 - \lambda^3) = 0$ with the three solutions $\lambda_{1,2,3} = \exp(i2\pi/3)$, $\exp(i4\pi/3)$, $\exp(i2\pi)$. Since $|\lambda_{1,2,3}| = 1$, there is no growing solution and the motion is stable. With an electron cloud, but without pinch and without space charge, we would have $\bar{X} \neq 0$ and $\bar{B} = \bar{X} = 0$. We note that the terms representing the tune variation along the bunch, $\bar{C}$ and $\bar{X}$, only enter in second order.

We find the solution to the general equation $p(\lambda) = 0$ numerically.

## 3.2 4 Particles

We now extend the model to 4 particles, in order to study the change in the growth rates with the number of particles considered. We naturally assume that each of the 4 model particles carries a charge $N_b e/4$ and we again take the same constant wake force $W_0$. Some particles now exchange their position after every 8th synchrotron period, where the average phases of different particles are different.

The longitudinal positions of the particles evolve as

$$z_1 = \hat{z}\cos\left(\frac{\omega_s s}{c}\right) \tag{32}$$

$$z_2 = \hat{z}\cos\left(\frac{\omega_s s}{c}+\frac{\pi}{4}\right) \tag{33}$$

$$z_3 = \hat{z}\cos\left(\frac{\omega_s s}{c}+2\pi\right) \tag{34}$$

$$z_4 = \hat{z}\cos\left(\frac{\omega_s s}{c}+\frac{3\pi}{2}\right) \tag{35}$$

where $\hat{z} \approx \sigma_z$.

We need to evaluate the equations of motion for a fourth period of the synchrotron oscillation. The solutions for the other 3 fourths then again follow by cyclic permutation. The initial ordering of the particles is (1,4,2,3). After an eight period it changes to (4,1,3,2), and, thereafter, to (4,3,1,2), etc. We solve the equation of motion for the first two eighths of a synchrotron period.

We proceed exactly as for the 3-particle model. Making similar approximations as before, Eq. (16) is replaced by

$$\begin{aligned}
&\tilde{y}_n\left(\frac{T_s c}{8}\right) \qquad (36)\\
&\approx \tilde{y}_n(0) + iD_4 \sum_{n',z_{n'}>z_n} \tilde{y}_{n'}\left[\frac{\pi c}{4\omega_s}\right.\\
&-i\left(\frac{a\omega_{\beta,0}c}{\omega_s^2}\right)\left[\cos\left(\pi/4+\phi_{n',0}\right)-\cos\phi_{n',0}\right]\\
&-\frac{i}{8}\left(\frac{b\omega_{\beta,0}c}{\omega_s^2}\right)\left[\cos\left(\pi/2+2\phi_{n',0}\right)-\cos 2\phi_{n',0}\right]\\
&+i\left(\frac{a\omega_{\beta,0}c}{\omega_s^2}\right)\left[\cos\left(\pi/4+\phi_{n,0}\right)-\cos\phi_{n,0}\right]\\
&\left.+\frac{i}{8}\left(\frac{b\omega_{\beta,0}c}{\omega_s^2}\right)\left[\cos\left(\pi/2+2\phi_{n,0}\right)-\cos 2\phi_{n,0}\right]\right].
\end{aligned}$$

where we have adjusted the definition of $D$ to the reduced particle charge:

$$D_4 \equiv \frac{N r_0 W_0 c}{8\gamma C \omega_\beta}. \tag{37}$$

$$\bar{C}_4 \equiv D_4\,\frac{\pi c}{4\omega_s} \tag{38}$$

$$\bar{A}_4 \equiv D_4\,\frac{a\omega_{\beta,0}c}{\omega_s^2} \tag{39}$$

$$\bar{B}_4 \equiv D_4\,\frac{b\omega_{\beta,0}c}{8\omega_s^2}, \tag{40}$$

Explicitly, the Eq. (36) amounts to

$$\begin{aligned}
\tilde{y}_1(\pi/4) &\approx \tilde{y}_1(0) \qquad (41)\\
\tilde{y}_4(\pi/4) &\approx \tilde{y}_4(0) + \tilde{y}_1(0)\left[i\bar{C}_4 - 1\bar{A}_4 - 2\bar{B}_4\right]\\
\tilde{y}_2(\pi/4) &\approx \tilde{y}_2(0) + \tilde{y}_1(0)\left[i\bar{C}_4 + (\sqrt{2}-1)\bar{A}_4\right]\\
&\quad + \tilde{y}_4(0)\left[i\bar{C}_4 + \sqrt{2}\bar{A}_4 + 2\bar{B}_4\right]\\
\tilde{y}_3(\pi/4) &\approx \tilde{y}_3(0) + \tilde{y}_1(0)\left[i\bar{C}_4 + (\sqrt{2}-2)\bar{A}_4\right]\\
&\quad + \tilde{y}_4(0)\left[i\bar{C}_4 + (\sqrt{2}-1)\bar{A}_4 + 2\bar{B}_4\right]\\
&\quad + \tilde{y}_2(0)\left[i\bar{C}_4 - \bar{A}_4\right]
\end{aligned}$$

The corresponding equations for the second eight synchrotron period are

$$\begin{aligned}
\tilde{y}_4(\pi/2) &\approx \tilde{y}_4(\pi/4) \qquad (42)\\
\tilde{y}_1(\pi/2) &\approx \tilde{y}_1(\pi/4) + \tilde{y}_4(0)\left[i\bar{C}_4 + \bar{A}_4 + 2\bar{B}_4\right]\\
\tilde{y}_3(\pi/2) &\approx \tilde{y}_3(\pi/4) + \tilde{y}_4(\pi/4)\left[i\bar{C}_4 + (1-\sqrt{2})\bar{A}_4\right.\\
&\quad \left.+2\bar{B}_4\right] + \tilde{y}_1(\pi/4)\left[i\bar{C}_4 - \sqrt{2}\bar{A}_4\right]\\
\tilde{y}_2(\pi/2) &\approx \tilde{y}_2(\pi/4) + \tilde{y}_4(\pi/4)\left[i\bar{C}_4 + 1\bar{A}_4\right]\\
&\quad + \tilde{y}_1(\pi/4)\left[i\bar{C}_4 - 2\bar{B}_4\right]\\
&\quad + \tilde{y}_3(\pi/4)\left[i\bar{C}_4 + \sqrt{2}\bar{A}_4 - 2\bar{B}_4\right]
\end{aligned}$$

As before, we can rewrite these transformations as a matrix equations relating the initial and final (4-component) amplitude vectors $\vec{y}_4(s) \equiv (\bar{y}_1(s), \bar{y}_2(s), \bar{y}_3(s), \bar{y}_4(s))$,

$$\vec{y}_4(\pi/4) = \mathbf{M}_{\pi/4}\vec{y}_4(0) \tag{43}$$

and

$$\vec{y}_4(\pi/2) = \mathbf{M}_{\pi/2}\vec{y}_4(\pi/4). \tag{44}$$

According to Eqs. (20) and (21), the matrices $\mathbf{M}_{\pi/4}$ and $\mathbf{M}_{\pi/2}$ are

$$\mathbf{M}_{\pi/4} = \tag{45}$$
$$\begin{pmatrix} 1 & 0 & 0 & 0 \\ i\bar{C}_4 + (\sqrt{2}-1)\bar{A}_4 & 1 & 0 & i\bar{C}_4 + \sqrt{2}\bar{A}_4 + 2\bar{B}_4 \\ i\bar{C}_4 + (\sqrt{2}-2)\bar{A}_4 & i\bar{C}_4 - \bar{A}_4 & 1 & i\bar{C}_4 + (\sqrt{2}-1)\bar{A}_4 + 2\bar{B}_4 \\ i\bar{C}_4 - \bar{A}_4 - 2\bar{B}_4 & 0 & 0 & 1 \end{pmatrix}$$

and

$$\mathbf{M}_{\pi/2} = \tag{46}$$
$$\begin{pmatrix} 1 & 0 & 0 & i\bar{C}_4 + \bar{A}_4 + 2\bar{B}_4 \\ i\bar{C}_4 - 2\bar{B}_4 & 1 & i\bar{C}_4 + \sqrt{2}\bar{A}_4 - 2\bar{B}_4 & i\bar{C}_4 + \bar{A}_4 \\ i\bar{C}_4 - \sqrt{2}\bar{A}_4 & 0 & 1 & i\bar{C}_4 + (1-\sqrt{2})\bar{A}_4 + 2\bar{B}_4 \\ 0 & 0 & 0 & 1 \end{pmatrix}$$

The permutation matrix in this case is

$$\mathbf{P}_4 = \begin{pmatrix} 0 & 0 & 0 & 1 \\ 1 & 0 & 0 & 0 \\ 0 & 1 & 0 & 0 \\ 0 & 0 & 1 & 0 \end{pmatrix} \tag{47}$$

and the total matrix for one full synchrotron period is obtained by taking the 4th power of the product matrix

$$\mathbf{M}_{4,\mathrm{tot}} \equiv (\mathbf{P}_4 \mathbf{M}_{\pi/2} \mathbf{M}_{\pi/4})^4. \tag{48}$$

We now need to determine the eigenvalues of

$$\mathbf{M}_{1/4} \equiv \mathbf{P}_4 \mathbf{M}_{\pi/2} \mathbf{M}_{\pi/4}, \tag{49}$$

which can be computed numerically.

### *3.3 Application to the CERN SPS*

We use typical SPS parameters listed in Table 1 and approximate the wake field as constant [2],

$$W_0 = \frac{8\pi\rho_e C}{N_b}, \tag{50}$$

the centroid tune shift due to the electron cloud

$$\Delta Q_{\mathrm{ec}} \approx \frac{r_p}{2\gamma}\beta_y \rho_e C \tag{51}$$

where $C$ is the ring circumference, and the space-charge tune shift

$$\Delta Q_{\mathrm{sc}} \approx -\frac{\beta_y r_p C N_b}{\gamma^3 (2\pi)^{3/2}\gamma^3 \sigma_z \sigma_y (\sigma_x + \sigma_y)}. \tag{52}$$

We start by evaluating the expressions derived from the 3-particle model. Inserting all the definitions, we have

$$\bar{C} = \frac{4\pi^2 \rho_e r_p c^2}{9\omega_s \gamma \omega_\beta} \tag{53}$$

$$\bar{A} \approx \frac{4\pi\rho_e r_p c^2}{3\gamma\omega_s^2}\left(\frac{\Delta Q}{Q}\right)_{\mathrm{ec}} \tag{54}$$

$$\bar{B} \approx \frac{\pi\rho_e r_p c^2}{6\gamma\omega_s^2}\left(\frac{\Delta Q}{Q}\right)_{\mathrm{sc}}, \tag{55}$$

where we have approximated $\omega_\beta \approx \omega_{\beta,0}$ and used the equality $\Delta\omega_\beta/\omega_\beta = \Delta Q/Q$ (the symbol $Q$ denotes the betatron tune).

Assuming the parameter values of Table 1, we then obtain $W_0 \approx 2 \times 10^6\ \mathrm{m}^{-2}$, $\Delta Q_{\mathrm{ec}} \approx 0.008$, $\Delta Q_{\mathrm{sc}} \approx 0.037$, and

$$\bar{C} \approx 2.4 \tag{56}$$

$$\bar{A} \approx -3.8 \tag{57}$$

$$\bar{B} \approx 2.3 \tag{58}$$

For the nominal SPS parameters, the two coefficients multiplying the sinusoidal functions in the expression for $\Delta\phi_i(s)$, Eq. (11), are almost equal to 2, and, hence, the linear expansion of the exponential in Eq. (16), which assumes $|\Delta\phi_n - \Delta\phi_{n'}|$ to be much smaller than 1, is not a good approximation. As mentioned earlier, this problem could be overcome by numerically computing the integrals in Eq. (16). In that case one might also replace the constant wake field by a more accurate resonator approximation, or even by a simulated wake field. However, we do not pursue these questions in the present report, and simply evaluate the formulae which we have derived above. We expect that this still gives a meaningful estimate of the instability growth rate and of its qualitative dependence on various parameters, since for tune shifts 3 or 4 times smaller than nominal, our treatment is perfectly valid. The formulae would also be valid with the nominal tune shifts but a higher synchrotron tune, *e.g.*, for the B factories.

We first numerically solve the equation $p(\lambda) = 0$ for a case with the electron-cloud wake field $W_0 \neq 0$, but without the electron pinch and the space charge tune shifts, *i.e.*, we consider $\bar{C} = 2.4$, $\bar{B} = 0$, $\bar{A} = 0$. The magnitude of the maximum eigenvalue is $|\lambda|_{\max} \approx 6.65$. The corresponding instability rise time is

$$\tau = \frac{T_s/3}{\ln|\lambda|_{\max}}, \tag{59}$$

which yields about 0.88 ms. The factor 3 enters, since we analyse the matrix describing the amplitude evolution over a third of the synchrotron period $T_s$.

Next, we include the tune variation due to the electron pinch, *i.e.*, we compute the eigenvalue for $\bar{C} = 2.4$, $\bar{B} = 0$, $\bar{A} = -3.8$, and find $|\lambda| \approx 6.69$ and still $\tau \approx 0.88$ ms.

Finally, we also add the space-charge force, *i.e.*, $\bar{C} = 2.4$, $\bar{B} = 2.3$, $\bar{A} = -3.8$, which yields $|\lambda| \approx 6.19$ or $\tau \approx 0.91$ ms. The addition of the space charge decreases the growth rate by about 7%. However, if we assume a larger value for the tune shift $-\Delta Q_{\mathrm{sc}}$, the growth rate increases.

Next, we perform the same calculations for the 4-particle model. In this case, with wake field only, $\bar{C}_4 = 1.80$, we have $|\lambda|_{\max} = 6.31$ or $\tau = 0.68$ ms; with wake field and electron pinch, $\bar{C}_4 = 1.80$, $\bar{A}_4 = -2.87$, we find $|\lambda|_{\max} = 5.75$ or $\tau = 0.71$ ms; and with wake field, electron pinch and space charge, $\bar{C}_4 = 1.80$, $\bar{A}_4 = -2.87$, $\bar{B}_4 = 1.71$, we obtain $|\lambda|_{\max} = 6.71$ or $\tau = 0.66$ ms. Thus, in the 4-particle model, the space charge reduces the rise time by about 8%.

We have also computed the eigenvectors for the different cases. The components of the eigenvector corresponding to the largest eigenvalue are large for the particles 2 and 3, in the 3-particle model, and for particles 3 and 4, in the 4-particle model. In both models the relative phase shift between the last and the second last particle reverses, if space charge detuning is included. With space charge the oscillation phase of the last particle is lagging behind that of the second last. Without space charge it is the opposite.

In other words, our simplified 3 and 4-particle models indeed suggest that the tune shift variation along the bunch due to space charge may change the instability growth rate and possibly the instability pattern. The predictions of the 4-particle model appear closer to the simulation results of Section 2 than those of the 3-particle model.

To better understand the difference between the 3 and 4-particle models, we have explored a larger range of space-charge tune shifts $\Delta Q_{\mathrm{sc}}$. Figure 6 illustrates the change in the instability rise time with $\Delta q_{\mathrm{sc}}$, which is predicted by

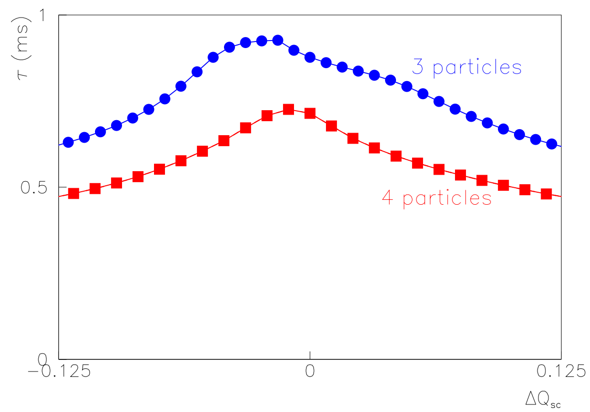


Figure 6: Instability rise time vs. maximum space-charge tune shift $\Delta Q_{\rm sc}$, for the SPS parameters of Table 1, assuming a constant electron-cloud wake field $W_0 \approx 1.7 \times 10^6$ m$^{-2}$, which corresponds to $\rho_e \approx 10^{12}$ m$^{-4}$, and an electron pinch resulting in $\Delta Q_{\rm ec} \approx 0.0077$ at the center of the bunch. Physical space-charge tune shifts correspond to negative values of $\Delta Q_{\rm sc}$; positive values would model the beam-beam interaction in an e$^+$e$^-$ or p$\bar{\rm p}$ collider.

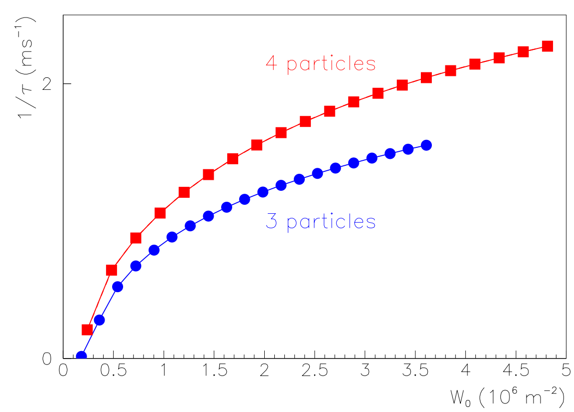


Figure 7: Growth rate vs. strength of electron wake-field $W_0$, for the SPS parameters of Table 1, without electron pinch and without space charge.

the two models, if we keep all other parameters constant. Again we see that the additional parabolic tune variation due to the space-charge force can have a noticeable effect, and it acts destabilizing over most of the parameter range, and, in particular, for the model using a larger number of particles. This appears consistent with the computer simulations. Increasing the number of model particles from 3 to 4 shifts the value of $\Delta Q_{\rm sc}$ where the maximum rise time is assumed towards 0, and it also decreases the predicted rise time for all values of $\Delta Q_{\rm sc}$.

It has been remarked by K. Oide [6] that the 3 or 4-particle model does not predict any threshold current or threshold impedance. This is also true if there is only a wake field but no pinch and no space charge, *i.e.*, for $\bar{A} = 0$, $\bar{B} = 0$, and $\bar{C} \neq 0$.

By contrast, an exact threshold is always found in standard mode-coupling calculations based on a perturbative solution of the Vlasov equation, which consider a continuous beam distribution, and also in a 2-particle model [4]. Figure 7 displays the growth rates predicted by the 3 and 4-particle models as a function of the wake-field strength. The figure suggests that for an increasing number of model-particles the growth rate approaches a threshold near $W_0 \approx 2 \times 10^5$ m$^{-2}$. For comparisom, the exact threshold predicted by the 2-particle model occurs at [4]

$$W_0^{\rm thr,2} = \frac{8\gamma C \omega_{\beta,0}\omega_s}{\pi r_p c^2 N_b}, \qquad (60)$$

which, in our example, yields $W_0^{\rm thr,2} \approx 3.3 \times 10^5$ m$^{-2}$, about 30% higher than the approximate threshold obtained for 3 or 4 particles.

## 4 CONCLUSION

Transverse space-charge forces and the beam-beam collision both introduce a Gaussian variation of the betatron tune along the bunch. Computer simulations of the single-bunch electron-cloud instability show that including this tune variation may enhance and alter the instability driven by the electron cloud.

In order to explore possible mechanisms by which the tune variation may affect the instability, we have developed two analytical few-particle models. In these models, we represent the bunch by either 3 or 4 particles, the electron cloud by a constant wake field and by a linear tune change along the bunch, and the space charge (or beam-beam interaction) by a parabolic tune change. Both models show that the space-charge or beam-beam tune shift may act destabilizing, in a large range of the parameter space. The agreement between the analytical model and simulation appears to improve with an increasing number of model particles.

Finally, in both few-particle models, the sign of the parabolic tune shift that would represent a beam-beam interaction for oppositely charged bunches results in slightly faster instabilities than the other sign corresponding to the space-charge tune shift, but the difference appears to decrease with the number of model particles.

## 5 ACKNOWLEDGEMENTS

We thank G. Arduini, K. Cornelis, H. Fukuma, M. Jimenez, S.-I. Kurokawa, K. Ohmi, K. Oide, E. Perevedentsev, and F. Ruggiero for helpful discussions and support.

## 6 REFERENCES

[1] G. Rumolo, F. Zimmermann, programme documentation at *http://wwwslap.cern.ch/collective/electron-cloud/electron-cloud.html*

[2] K. Ohmi and F. Zimmermann, “Head-Tail Instability caused by Electron Cloud in Positron Storage Rings”, Phys. Rev. Letters 85, p. 3821 (2000).

[3] G. Rumolo, F. Zimmermann, “Simulation of Single Bunch Instabilities Driven by Electron Cloud in the SPS,” Proc. PAC’2001 Chicago, USA, and CERN-SL-2001-041 (AP) (2001).

[4] A. Chao, “Physics of Collective Beam Instabilities in High Energy Accelerators,” John Wiley, New York (1993).

[5] K. Cornelis, private communication (2001).

[6] K. Oide, private communication (2001).